



Submitted to

International Conference on High Energy Physics, ICHEP 2004, August 16-22, 2004, Beijing
(Abstract **5-0170** Parallel Session **5**)

www-h1.desy.de/h1/www/publications/conf/conf_list.html

Measurement of the Inclusive DIS Cross Section at Low Q^2 and High x using Events with Initial State Radiation

H1 Collaboration

Abstract

The inclusive DIS cross section is measured at low Q^2 and relatively large x using events with initial state photon radiation from the incoming electron. In this analysis the radiated photon is not explicitly detected. Instead its energy is inferred from a longitudinal momentum imbalance, such that the energy of the interacting electron and the event kinematics can be reconstructed. The neutral current cross section is thus measured for $0.35 \leq Q^2 \leq 0.85 \text{ GeV}^2$ and $10^{-4} \lesssim x \lesssim 5 \cdot 10^{-3}$.

1 Introduction

The region of momentum transfer squared Q^2 around 1 GeV^2 deserves particular attention because it corresponds to the transition between the non-perturbative and the perturbative domains in deep-inelastic scattering (DIS). Thus at HERA a special electron-proton scattering run was performed in which the interaction vertex was shifted by about 70 cm in the proton beam direction which allows larger electron scattering angles¹ θ_e and thus lower values of Q^2 to be accessed.

The data presented here were taken in August 2000 and correspond to a luminosity of 0.6 pb^{-1} . The results represent an extension to our previous measurements [1] of inclusive DIS cross sections at $Q^2 \lesssim 1 \text{ GeV}^2$ based on the same data. In this analysis, an extension to larger x values at low Q^2 is achieved by making use of events with initial state photon radiation (ISR) from the incoming electron. The photon radiation results in a reduced incoming electron energy, such that the ep centre of mass energy is reduced and larger values of x are accessed at fixed Q^2 than is the case for non-radiative events. The kinematic plane and its extension with the new analysis is illustrated in Figure 1.

The inclusive measurements determine the cross section which at low Q^2 , in the one-photon exchange approximation, can be written in reduced form as

$$\frac{Q^4 x}{2\pi\alpha^2 Y_+} \cdot \frac{d^2\sigma}{dx dQ^2} = \sigma_r = F_2(x, Q^2) - \frac{y^2}{Y_+} \cdot F_L(x, Q^2). \quad (1)$$

Here y is the inelasticity which is related to x and Q^2 as $y = Q^2/sx$. The beam energies determine the centre of mass energy squared, $s = 4E_e E_p$, and Y_+ is defined as $1 + (1 - y)^2$. In the region of inelasticity below $y = 0.6$ the contribution of the longitudinal structure function $F_L(x, Q^2)$ is small due to the kinematic factor y^2/Y_+ and since $F_L \leq F_2$. Thus the measurement of σ_r at lower y directly determines F_2 with a small correction for F_L .

2 Experimental Methods

2.1 Kinematic Reconstruction

In contrast to earlier ISR analyses [2], this analysis does not require the observation of the radiated photon. Instead, its presence is inferred from energy and longitudinal momentum conservation. Assuming that the photon is radiated collinear with the electron beam, the energy E_γ of the radiated photon is then given by $2E_\gamma = 2E_e^0 - (E - p_z)_{e'} - (E - p_z)_h$, where $E_e^0 = 27.6 \text{ GeV}$ is the electron beam energy, $(E - p_z)_{e'}$ is the measured difference between the energy and the longitudinal momentum of the scattered electron and $(E - p_z)_h$ is the same quantity for the full hadronic final state. The reduced incoming electron beam energy E_e is then given by $E_e = E_e^0 - E_\gamma$. The reconstruction of y and Q^2 proceeds using the ‘ Σ method’,

¹Note that the polar angles θ are defined with respect to the proton beam direction.

which relies on $\Sigma = (E - p_z)_h$. The reconstruction of x is then performed in a manner that is independent of the electron beam energy E_e^0 . The kinematics are reconstructed using

$$y_\Sigma = \frac{\Sigma}{\Sigma + E_{e'}(1 - \cos \theta_e)} \quad Q_\Sigma^2 = \frac{E_{e'}^2 \sin^2 \theta_e}{1 - y_\Sigma} \quad x_R = \frac{Q_\Sigma^2}{2\Sigma E_p}$$

where θ_e is the electron scattering angle.

The scattered electron energy E_e' is measured in the backward electromagnetic lead scintillating fibre calorimeter SPACAL [3]. The polar angle θ_e is measured in the Backward Silicon Tracker (BST) [4, 5, 6]. The hadronic final state is reconstructed in the Liquid Argon calorimeter (LAr) and the SPACAL [7].

2.2 Triggers and Event Selection

The data are triggered using the local energy sums in the SPACAL calorimeter with an energy threshold set to 6 GeV. Low energy deposits can also be caused by hadrons and photons from events at very low $Q^2 \ll 1 \text{ GeV}^2$ which mimic an electron signal in the SPACAL. Part of these photoproduction background events is recognised by tagging a scattered electron at very small angles in the electron tagger calorimeter upstream the electron beam.

The efficiency of all trigger elements exceeds 98% and is controlled by independent tracking triggers to an accuracy of 0.5%. From a monitor event sample, defined by a vertex accurately reconstructed in the central tracker and by a high energy SPACAL cluster, the BST efficiency is determined and the Monte-Carlo simulation correspondingly adjusted. The hit efficiency of the BST is 97% on average, excluding a few malfunctioning sensor modules.

DIS events are required to have a vertex reconstructed from a track measured in the BST and its intersection with the beam axis. The track has to be associated to the highest energetic cluster in the SPACAL, where the cluster is required to extend by less than two Molière radii in the transverse plane. Any energy behind the electromagnetic cluster measured in the hadronic SPACAL may not exceed a small fraction of E_e' . The criteria of the DIS event selection are summarised in Table 1. The selection is identical to the selection from the standard analysis

z vertex position	$ z - 70 < 45\text{cm}$
SPACAL cluster radius	$< 4\text{cm}$
SPACAL-BST matching	$\delta r < 2\text{cm}$
electromagnetic SPACAL energy	$> 7 \text{ GeV}$
hadronic SPACAL energy	$< 15\% \text{ of } E_e'$

Table 1: *Basic criteria to select DIS events.*

[1], with the exception of the $E - p_z$ cut, which in the previous analysis was used in order to remove radiative events.

A high statistics simulation of DIS events is performed using the program DJANGO [8] with a parameterisation of the parton distributions (MRST 3,75) [9] extended to very low Q^2 . For the extraction of the cross section and comparisons of experimental with simulated spectra, a recent

fit to previous low Q^2 data [10, 11] was used for reweighting which is based on the fractal proton structure concept. This fit [12] describes the data in the non-perturbative region and the data in the deep-inelastic domain very well. Photoproduction events are simulated with the program PHOJET [13]. The simulated events are subject to the same reconstruction and analysis chain as the real data. In the comparisons of experimental distributions with the Monte-Carlo spectra, these are normalised to the measured luminosity.

The luminosity as determined from the cross section of the elastic bremsstrahlung process is measured with a precision of 1.8%.

Other analysis details like alignment and calibration of the detector can be found elsewhere [1].

2.3 Control Plots

Control distributions corresponding to the measured ISR-dominated phase space are shown in figure 2. There is good agreement between the observed uncorrected data distributions and the expectation based on a DJANGO simulation of inclusive DIS together with a PHOJET simulation of the photoproduction background.

2.4 Systematic Uncertainties

The total systematic error of the cross section measurement with ISR events is about 10%. The main uncertainties and their contributions to the cross section error are:

- correlated systematic errors:
 - electron energy uncertainty – up to 2% for low energy electrons,
 - error of electron angle measurement with BST – about 2% ,
 - hadronic energy uncertainty – about 4% ,
 - photoproduction background uncertainty extend to 5% at low energy ,
- uncorrelated systematic errors:
 - Monte Carlo statistics – 4%,
 - BST reconstruction efficiency – 2%,
 - radiative corrections – 2%,
 - trigger inefficiency – 0.5%.

3 Results

3.1 Cross Section and the Proton Structure Function F_2

The kinematic region accessed in this measurement is divided into four Q^2 intervals. The data are also divided in bins of y . The binning is adapted to the resolution in the measurement of the kinematic variables. Bins are accepted if the purity and stability are bigger than 30%. Here the purity (stability) is defined as the number of simulated events which originate from a bin and which are reconstructed in it, divided by the number of reconstructed (generated) events in that bin.

Figure 3 shows the resulting measurements, expressed in the form of the reduced cross section. The data points cover the region $0.35 \leq Q^2 \leq 0.85 \text{ GeV}^2$ and $10^{-4} \lesssim x \lesssim 5 \cdot 10^{-3}$. They are compared with the extrapolated predictions of a fit for F_2 based on a self-similar structure to the proton (FRACTAL FIT F_2) [12], to which an F_L term has been added, based on a dipole model [14]. They are also compared with the results from a parameterisation (ALLM97 F_2) [15] of inclusive and exclusive DIS and photoproduction data. All predictions are in good agreement with the data.

The extension in kinematic phase space achieved using the new method is illustrated in figure 4, where the present data are compared with the results from the non-radiative shifted vertex analysis [1]. Figure 5 shows the overall status of DIS measurements in the low Q^2 region, including in addition data from the ZEUS beampipe tracker [11], from a further H1 measurement at low Q^2 and large x using QED-Compton events [16] and from NMC [17]. The new data are compatible with the previous measurements.

3.2 Rise of $F_2(x, Q^2)$ Towards Low x

Recently the H1 Collaboration has presented [19] a measurement of the derivative

$$\left(\frac{\partial \ln F_2(x, Q^2)}{\partial \ln x} \right)_{Q^2} \equiv -\lambda(x, Q^2) \quad (2)$$

which quantifies the behaviour of the rise of $F_2(x, Q^2)$ towards low x at fixed Q^2 . The new analysis allows improved extractions of the parameter λ . Figure 6 shows the results for λ obtained by fitting the current data at fixed Q^2 values, together with the previous shifted vertex measurements [1]. Also shown are H1 results from larger Q^2 values [18][19] and ZEUS results [11]. The new measurements confirm the change in behaviour of λ from a logarithmic dependence on Q^2 at large Q^2 to a weaker dependence compatible with reaching a constant consistent with the soft pomeron intercept as $Q^2 \rightarrow 0$. The change takes place on distance scales of the order of 0.3 fm and can be interpreted as being related to a transition from partonic to hadronic degrees of freedom.

4 Summary

A new measurement of the deep-inelastic electron-proton scattering cross section based on H1 data collected with the interaction vertex shifted by 70 cm is presented. The analysis introduces a novel method, which allows the previous analysis of this data set to be extended into the higher x region by means of events with initial state photon radiation from the incoming electron. The radiated photon is not explicitly detected, but its parameters are inferred from energy and momentum conservation. The neutral current cross section is thus measured for $0.35 \leq Q^2 \leq 0.85 \text{ GeV}^2$ and $10^{-4} \lesssim x \lesssim 5 \cdot 10^{-3}$. In the kinematic region of this measurement $F_2(x, Q^2)$ still rises towards low x at fixed Q^2 like $F_2(x, Q^2) = c(Q^2) \cdot x^{-\lambda(Q^2)}$. The new analysis allows improved extractions of the parameter λ from the H1 data.

Acknowledgements We are very grateful to the HERA machine group whose outstanding efforts made this experiment possible. We acknowledge the support of the DESY technical staff. We appreciate the substantial effort of the engineers and technicians who constructed and maintain the detector. We thank the funding agencies for financial support of this experiment. We wish to thank the DESY directorate for the support and hospitality extended to the non-DESY members of the collaboration.

References

- [1] H1 Collaboration, contributed paper 082 to EPS03, Aachen.
- [2] H1 Collaboration, contributed paper 976 to ICHEP02, Amsterdam.
- [3] R. Appuhn *et al.*, Nucl. Instr. and Meth. **A386** (1996) 397.
- [4] V.V. Arkadov, PhD Thesis, Berlin, Humboldt-University, 2000, DESY-Thesis-2000-046.
- [5] D. Eckstein, PhD Thesis, Berlin, Humboldt-University, 2002, DESY-Thesis-2002-008.
- [6] T. Laštovička, PhD Thesis, Berlin, Humboldt-University, 2004, DESY-Thesis-2004-016.
- [7] H1 Collaboration, I. Abt *et al.*, Nucl. Instr. and Meth. **A386** (1997) 310 and **A386** (1997) 348.
- [8] G. A. Schuler and H. Spiesberger, Proc. Workshop on HERA Physics, Vol 3, eds. W. Buchmüller and G. Ingelman, Hamburg, DESY (1992), p. 1419;
A. Kwiatkowski, H. Spiesberger and H.-J. Möhring, Comp. Phys. Comm. **69** (1992) 155;
L. Lönnblad, Comp. Phys. Comm. **71** (1992) 15.
- [9] PDFLIB: The Parton Density Functions Library, Version 8.04, MRST set 75, CERN.
- [10] H1 Collaboration, C. Adloff *et al.*, Eur. Phys. J. C **21** (2001) 33-61, [hep-ex/0012153].
- [11] ZEUS Collaboration, J. Breitweg *et al.*, Phys. Lett. B **487** (2000) 53.

- [12] T. Laštovička, Eur. Phys. J. C **24** (2002) 529 [hep-ph/0203260].
- [13] R. Engel and J. Ranft, Phys. Rev. **D54** (1996) 4244.
- [14] K. Golec-Biernat and M. Wüsthoff, Phys. Rev. D **59** (1999) 014017, [hep-ph/9807513].
- [15] H. Abramowicz and A. Levy, The ALLM parameterization of $\sigma(\text{tot})(\gamma^* p)$: An update, DESY-97-251, [hep-ph/9712415] (1997).
- [16] H1 Collaboration, contributed paper 084 to EPS03, Aachen.
- [17] NMC Collaboration, M. Arneodo *et al.*, Nucl. Phys. **B483** (1997) 3.
- [18] H1 Collaboration, Eur. Phys. J. C **21** (2001) 33 [hep-ex/0012153].
- [19] H1 Collaboration, C. Adloff *et al.*, Phys. Lett. B **520** (2001) 183 [hep-ex/0108035].

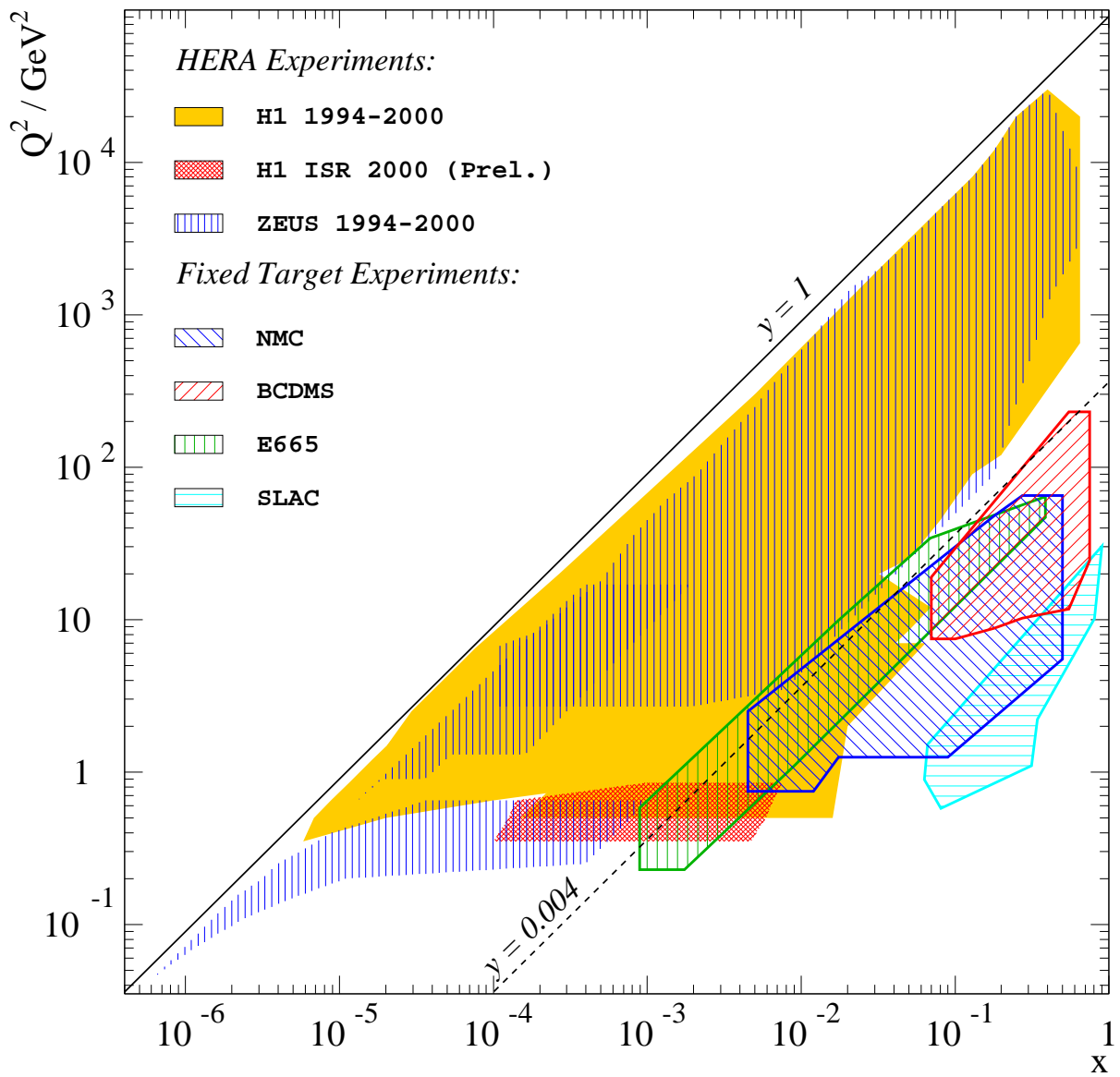


Figure 1: Kinematic region covered by F_2 measurements at HERA and fixed target experiments. The extension to higher x for low Q^2 region provided by the ISR events analysis shown.

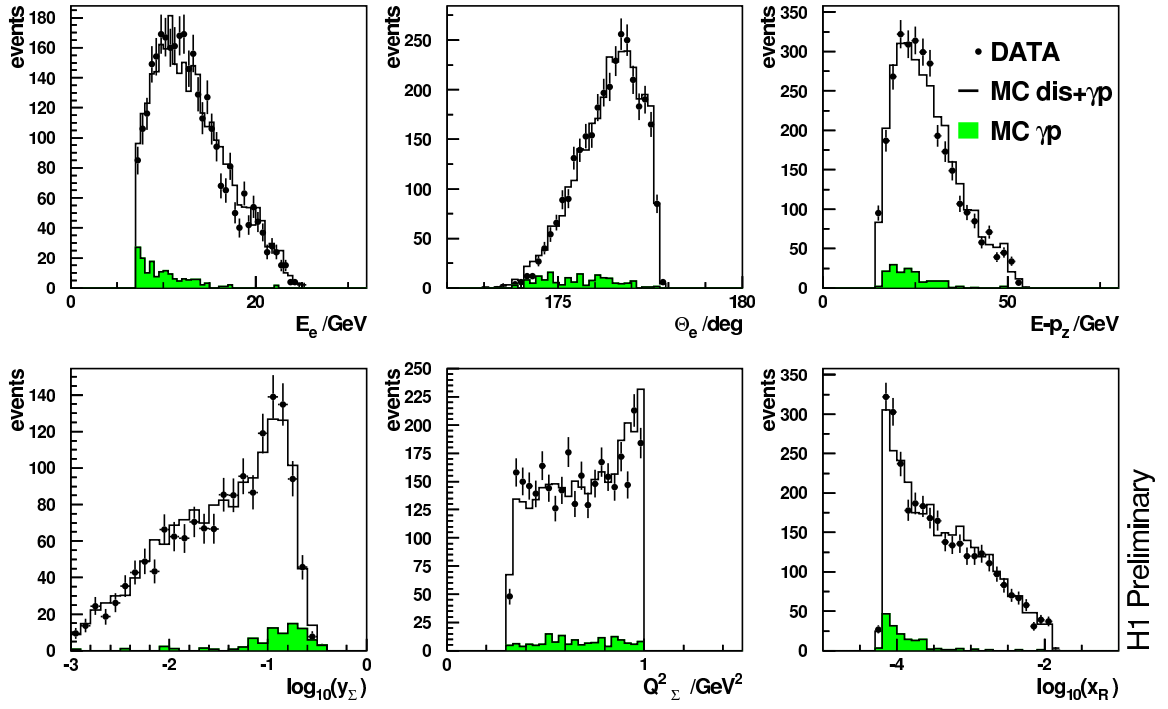


Figure 2: Control distributions for the ISR-dominated event selection. The uncorrected data distributions are compared with the sum of the DIS expectation (DJANGO Monte Carlo model) and the expected photoproduction background (PHOJET Monte Carlo model). The comparisons are shown for the effective incoming electron energy E_e , the electron scattering angle θ_e , the sum of the electron and hadron $E - p_z$ and the reconstructed y , Q^2 and x as used in the measurement.

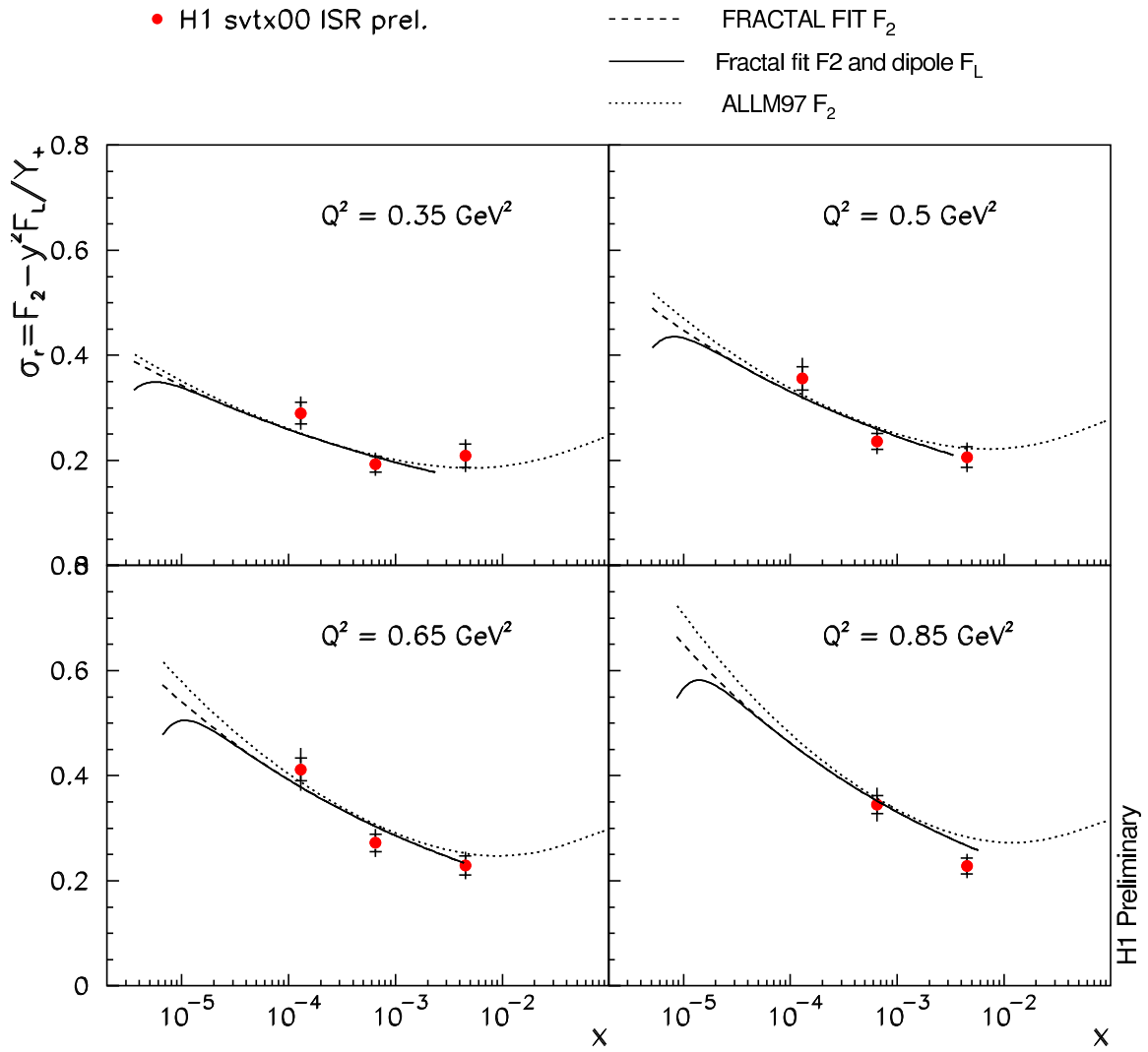


Figure 3: Measured reduced cross section from the shifted vertex ISR analysis, compared with the extrapolated predictions of a ‘fractal’ fit based on self-similar proton structure, with the sum of the fractal fit result for F_2 and a F_L contribution from a dipole model and with the ALLM97 parameterisation.

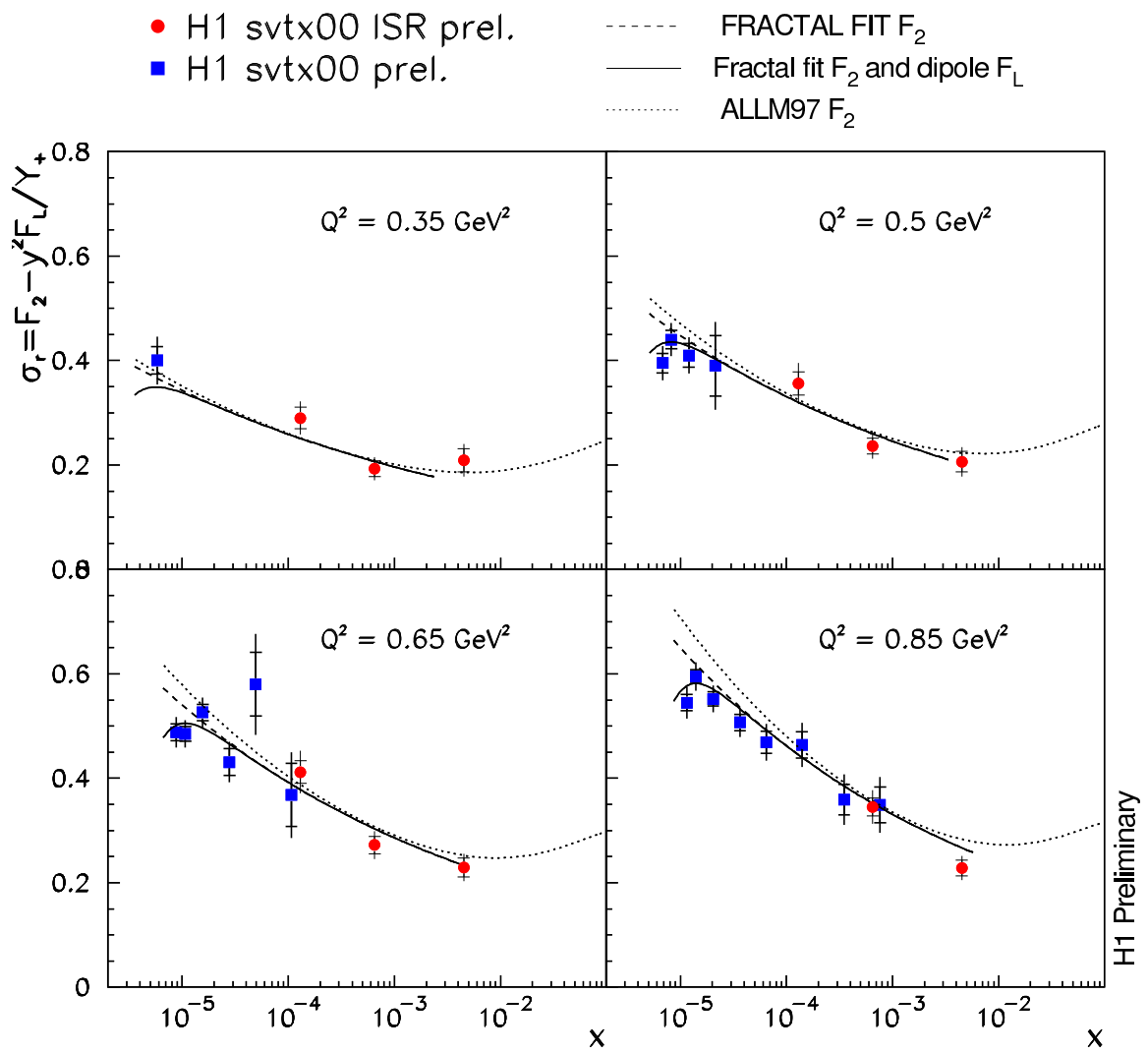


Figure 4: Measured reduced cross section from both ISR and non-radiative measurements using shifted vertex data.

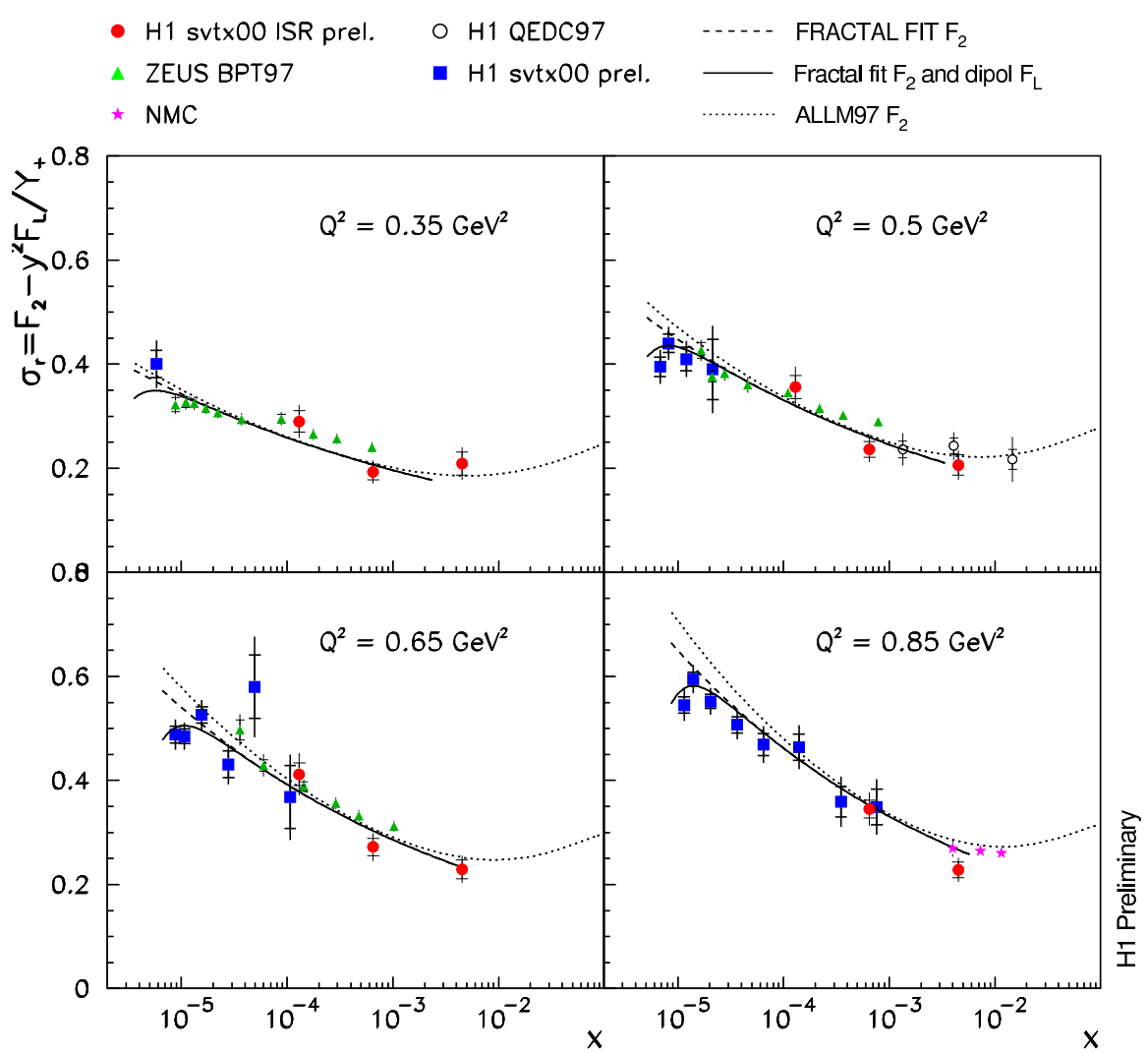


Figure 5: Compilation of reduced cross section measurements with $Q^2 < 1 \text{ GeV}^2$ from H1, ZEUS and NMC.

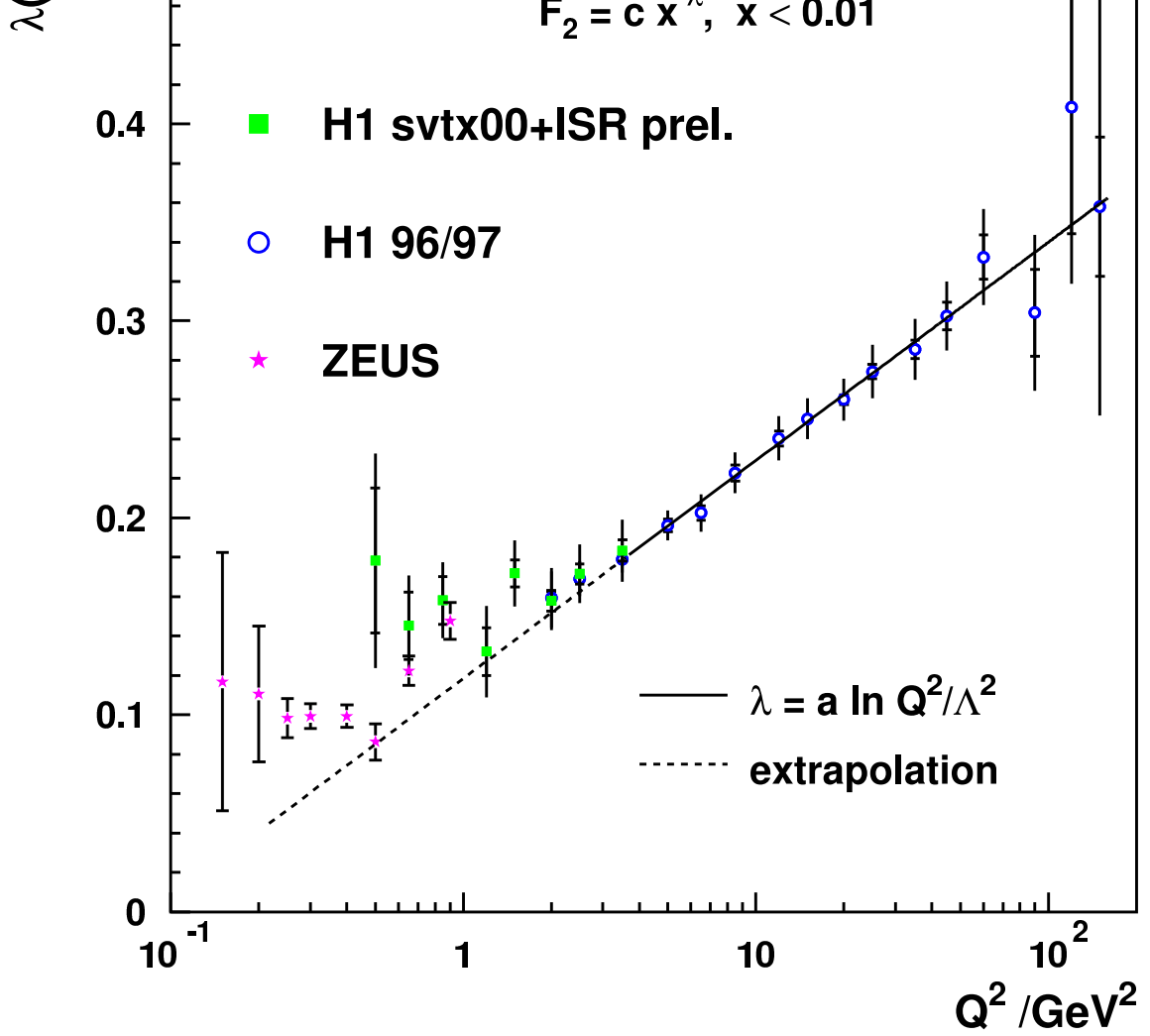


Figure 6: Compilation of selected HERA results on the parameter λ , obtained from fits of the form $F_2 = c(Q^2) \cdot x^{-\lambda(Q^2)}$ to low x data.